Dynamic behavior and seismic retrofitting method for half-through steel arch bridges subjected to fault displacement

Toshitaka Yamao
Dept. of Civil and Environmental Engineering, Kumamoto University, Kumamoto, Japan

Yoshie Tsujino
Obayashi Corporation Co. Ltd. Institution, Tokyo, Japan

Zhanfei Wang
Civil Engineering College, Shenyang Jianzhu University, Shenyang, China

ABSTRACT: This paper presents the seismic behavior of dynamic response analyses and seismic retrofitting of half-through steel arch bridges subjected to fault displacement. Both the 1999 Taiwan Ji-Ji Earthquake wave and the fault displacement wave obtained from the time integral of the acceleration response wave were applied and the response behavior was investigated. The dynamic response analyses were carried out using earthquake waves including fault displacement in transverse and longitudinal (expanding and shrinking) directions in order to investigate seismic behavior of bridge models. According to the analytical results, it was found that the plastic members were clustered near the intersections of arch ribs and stiffened girders and at the union of stiffened girders and end support. Finally, the effect of the proposed seismic retrofitting methods on the seismic behavior of the bridge model was discussed.

1 INTRODUCTION

When a strong earthquake occurs, steel arch bridges and steel bridge piers are frequently subjected to fault displacement induced by ground motion (Japan Society of Civil Engineering 1999a,b). Thus, it is still necessary to establish a method concerning the effect of fault displacement to check the seismic performance developed from nonlinear dynamic analysis for arch bridge design. Furthermore, it is needful to construct steel arch bridges possessing high seismic capacity at a minimum cost. Half-through type steel arch bridge is one of the arch bridges which reveal complicated behavior when subjected to ground motion or fault displacement and ground motion. However, seismic performance and failure behavior have not been yet clarified and only few studies concerning nonlinear seismic analysis when subjected to fault displacement have been reported (Yamao et al. 2007).

This paper presents the results of nonlinear dynamic response analysis of a half-through type steel arch bridge subjected to fault displacement including earthquake waves in transverse and longitudinal (expanding and shrinking) directions. In this study, the fault displacement induced by the ground motion was assumed to occur at the surface of the earth in the middle of the bridge span as shown in Fig.1. In dynamic response analyses, the loading conditions were adjusted by controlling two different fault displacement waves at both ends of stiffened girders and at both springings of arch ribs. That is, both the fault displacement wave obtained from the time integral of the acceleration response wave and the ground motion simulated from the 1999 Taiwan Ji-Ji Earthquake wave were input. The seismic behavior of the bridge model subjected to the fault displacement including ground motion was investigated. Finally, in order to control the seismic demand of a half-through steel arch bridge, the seismic retrofitting methods were proposed and we discussed the effect of the proposed method s on the seismic behavior of the bridge model.

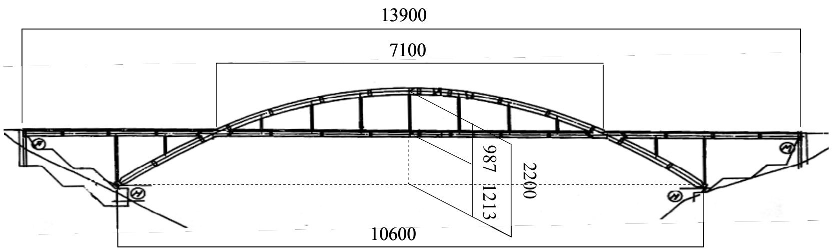

Figure 1 : Half-through arch bridge (unit: mm)

2 SEISMIC RESPONSE ANALYSIS

2.1 Theoretical arch model

The theoretical arch model studied herein is representative for actual half-through type arch bridges as shown in Fig.1.The theoretical model, in which 11 vertical columns are hinged to arch ribs at both ends. The arch has a span length (l) of 106 m and the arch rise (f) is 22 m. The global axis of the arch ribs are also shown in Fig.2(a),(b), where b and L represent the width of a stiffened girder and the deck span, respectively. The cross sectional profiles of vertical members and lateral members are rectangular and I-sections as shown in Figure 3(b) and 3(c). The model was assumed to have no residual stresses and initial crookedness modes. Material properties of the models used in the numerical analyses were assumed to be SM490Y steel type (JIS) with the yield stress (σ_y) of 353 MP_a and Young's modulus E was 206 GPa, respectively. Arch rise-to-span ratio (f/l) was taken to be 0.21 according to the condition of the actual arch bridges.

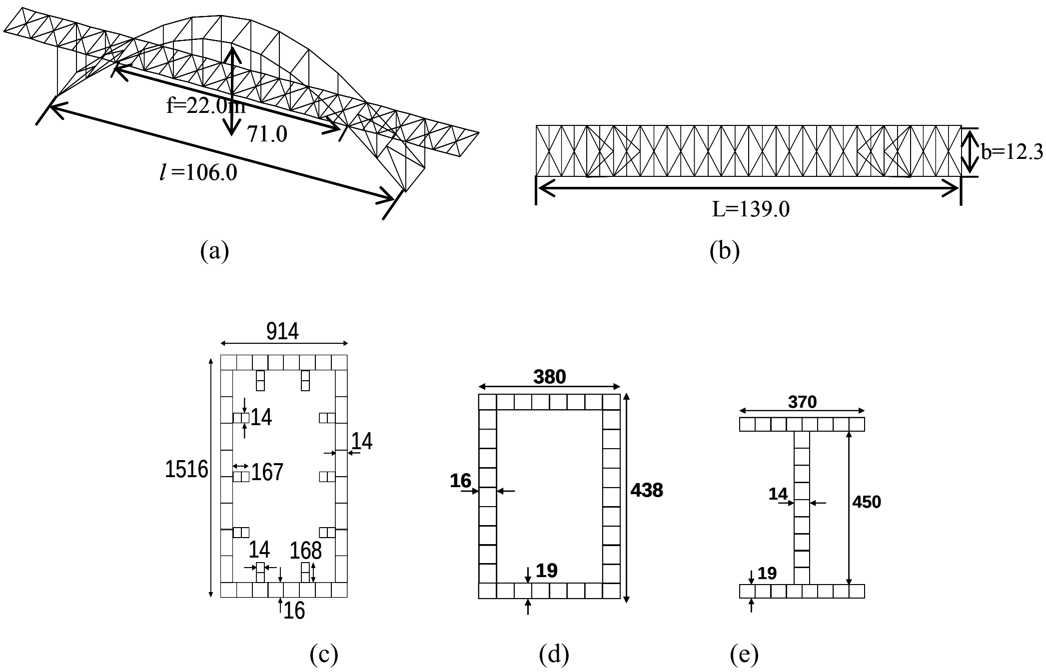

Figure 2 : Theoretical arch model (unit: m):(a)Global view of theoretical model, (b)Plane view of theoretical model, (c)Arch rib, (d)Vertical column, (e)Lateral member

2.2 Input seismic waves

The fault displacement wave used in this analysis was obtained from the time integral of the acceleration response wave, that is, the ground motion simulated from the 1999 Taiwan Ji-Ji Earthquake wave as shown in Fig.5. For the 1999 Taiwan Ji-Ji Earthquake input wave, the relative large fault displacement measured after the earthquake was also concerned. Fig.6(a) illustrates three fault displacement waves TCU68EW2-3, TCU68EW2-5 and TCU68EW2-6 and the residual displacements of these waves are different. Fig.6(b) shows the relative displacement curve for different two fault displacement waves and the maximum relative fault displacement is 3m. In the dynamic response analyses, both the seismic waves and the fault displacement wave were input in order to simulate the movement at both ends of stiffened girders and at both arch springing. In relative fault displacements 1m, the TCU68EW2-5 wave was applied at the left arch sprnging and the TCU68EW2-6 wave was applied at the right arch sprnging in longitudinal or transverse directions, as mentioned in Fig. 4, respectively. The relative fault displacement is changed 1-3m by combination of two fault displacement waves as shown in Fig.6(b).

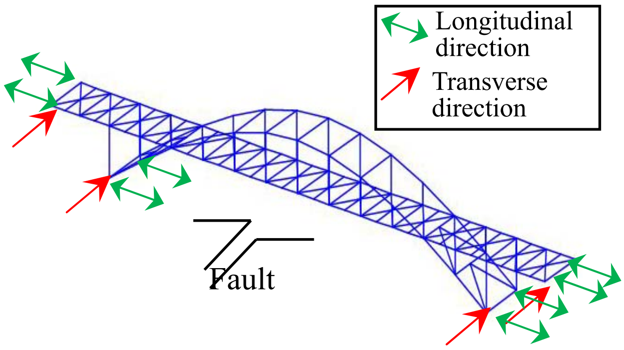

Figure 4 : Loading conditions in seismic fault displacement analysis

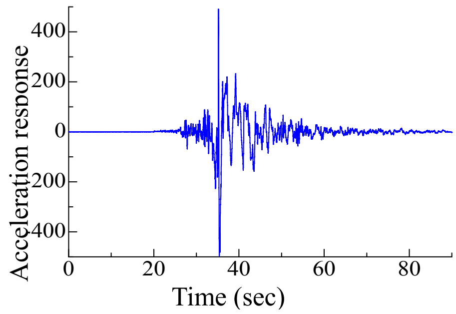

Figure 5 : 1999 Ji-Ji Earthquake wave

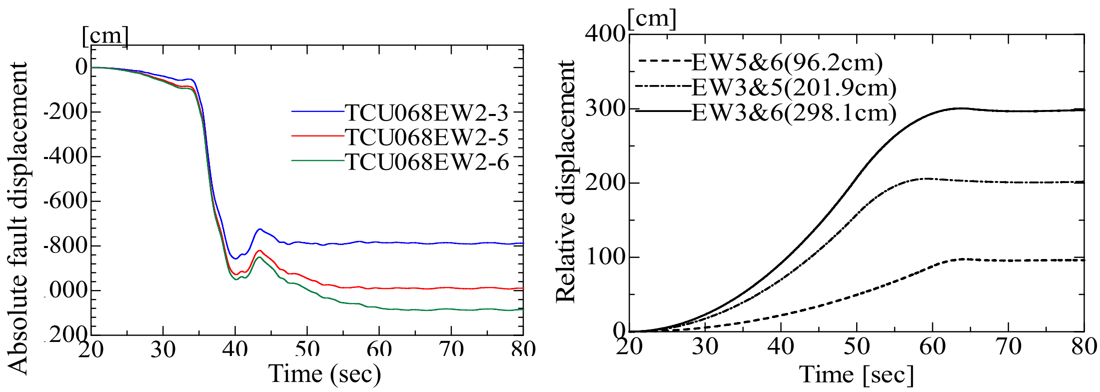

(a) (b)

Figure 6 : Input fault displacement wave:(a)Input fault displacement wave, (b)Relative displacement

2.3 Eigenvalue analysis

The eigenvalue analysis was carried out to investigate the effect of arch ribs and stiffened girders on the natural periods of the bridge model. In order to understand the fundamental dynamic characteristics, Table 1 presents the natural periods and the effective mass ratios of each predominant mode. The maximum effective mass ratios obtained in X, Y and Z directions imply the order of the dominant natural period. It can be seen from Table 1 that the arch bridge model is possible to vibrate sympathetically at the 1st mode in longitudinal direction (X-axis), 2th and 5th modes in transverse direction (Y-axis) and 8th mode in-plane direction (Z-axis), respectively.

Table 1 : Result of eigenvalue analysis

Order of period	Natural frequency(Hz)	Natural periods(sec)	Effective massratio (%)		
			X	Y	Z
1	1.1038	0.90593	39	0	0
2	1.8226	0.54866	0	37	0
3	3.2313	0.30948	0	0	0
4	3.5552	0.28128	11	0	0
5	3.7638	0.26569	0	40	0
6	4.1324	0.24199	0	5	0
7	4.3546	0.22964	0	0	0
8	4.594	0.21767	0	0	40
9	5.1533	0.19405	0	0	15
10	5.6619	0.17662	0	1	0

2.4 Damping matrix and numerical analysis

Numerical analyses were conducted using the Newmark-β method (β = 0.25) where the equations of motion were integrated with respect to time taking into account geometrical non-linearity. A constant time step of 0.001 sec and a damping model (Rayleigh type) calibrated to the initial stiffness and mass were utilized. The seismic response analysis with ground acceleration input and a constant dead load was performed using the nonlinear FEM program TDAPIII (NIPPON TDAPIII 2005), which is capable of taking into account material non-linearity.

3 RESPONSE BEHAVIOR OF FALUT DISPLACEMEENT

3.1 Distribution of plastic zones

Fig.7 illustrates the deformation modes of the arch bridge in longitudinal direction (expanding and shrinking) when 3.0 m relative displacement was applied. The yielded members corresponding to the deformation mode subjected to 1.0 m relative displacement are also illustrated in Fig.8. It can be seen that the plastic members are clustered beneath the joints of the arch ribs, end vertical columns and stiffened girders. This is caused by the large deformation at this intersection zones as shown in Fig.7. Fig.9 shows some element numbers of the theoretical model in order to illustrate the plastic ratios of strain for these members.

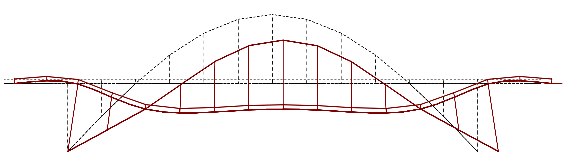

(a)

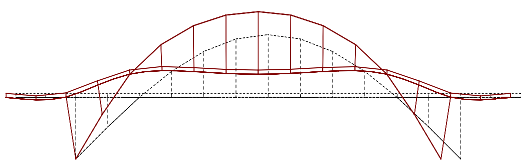

(b)

Figure 7 : Deformation modes of theoretical modeltic analysision dgeion. Direction:(a)Longitudinal directiong(Shrinking), (b)Longitudinal direction(Expanding)

3.2 Distribution of maximum and minimum plastic ratios of strain

Fig.10 shows the distribution of the maximum and the minimum plastic ratios of strain response of the arch rib and the stiffened girder in longitudinal direction. The strain ratio was plotted at 1.0m, 2.0m and 3.0m of relative displacement applied and non-dimensionalized parameter. The results coincide with the locations of yielded elements where the maximum strains of the arch rib occurred beneath the joints of the arch rib and the stiffened girder.

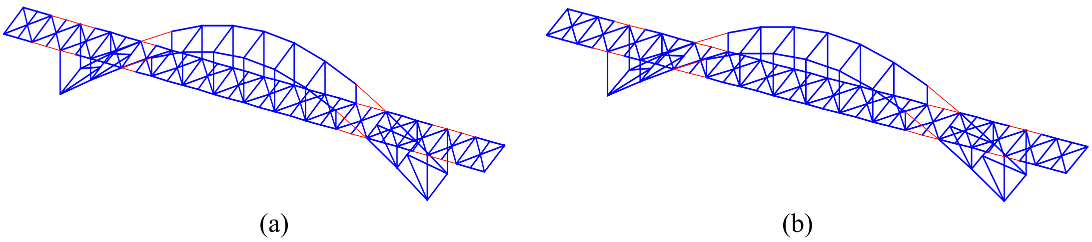

Figure 8 : Distributions of tic analysision dgeion.direction:(a) Longitudinal directiong(Shrinking), (b)Longitudinal direction(Expanding)

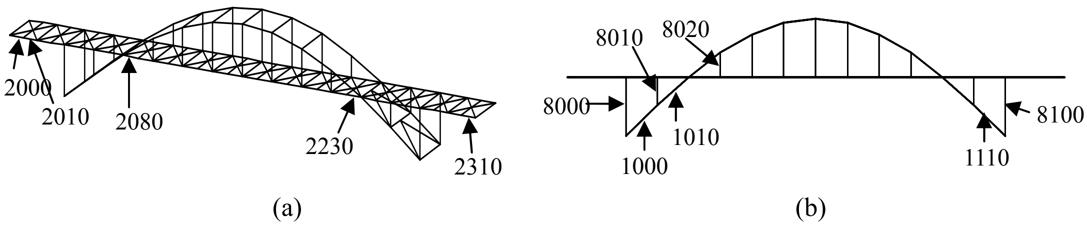

Figure 9 : Main element numbers of theoretical modeltic analysision dgeion direction(a)Arch rib and vertical columns, (b)Stiffened

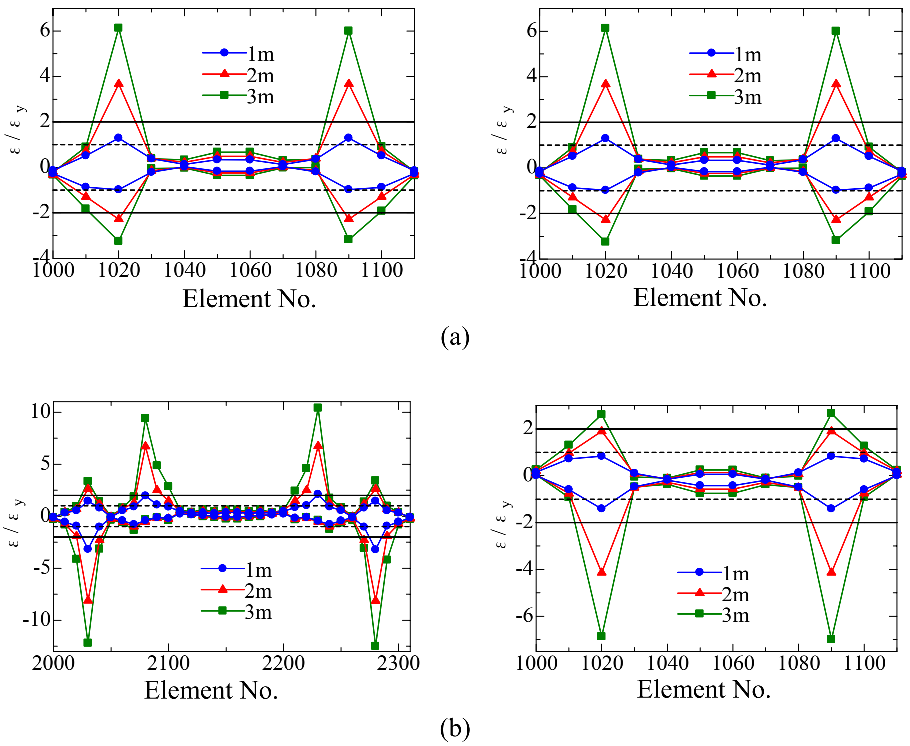

Figure 10 : Distribution of maximum and minimum plastic ratios of strain response in longitudinal direction : (a) Longitudinal direction (shrinking), (b) Longitudinal direction (expanding)

The distribution of the maximum and the minimum plastic ratios of strain response of the arch rib, the stiffened girder and vertical column in transverse direction were illustrated in Fig.11. From these figures, it was found that maximum and minimum strain ratios in transverse direction were relatively small and were nearly equal to 1.2. The results coincide also with the locations of yielded elements where the maximum strains of the arch rib occurred beneath the joints of the arch rib and the stiffened girder.

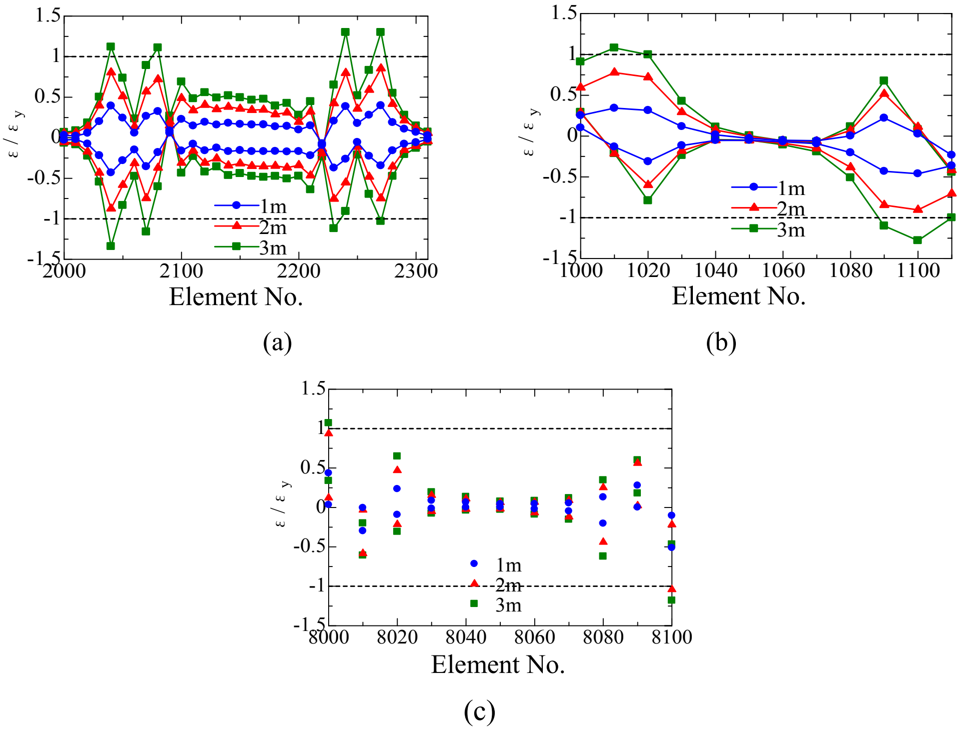

Figure 11 : Distributions of maximum and minimum plastic ratios of strain response in transverse direction:(a)Arch rib, (b)Stiffened girder, (c)Vertical column

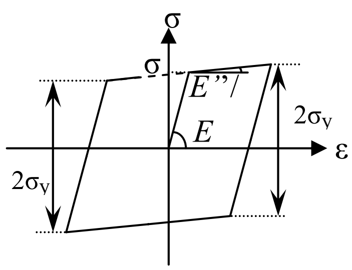

Figure 12 : Stress-strain relation of BRB

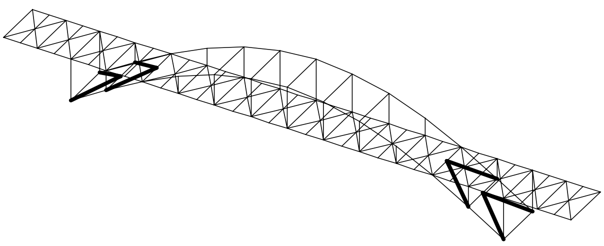

Figure 13 : Installed positions of BRB

Table 2 : Cross section area of BRB

	Yield stress [MPa]	Cross section area [cm^2]	Yield force [kN]
Original model	235	203.700	5,900
BRB	235	60.000	1,410

4 SEISMIC RETROFITTING METHOD OF HALF-THROUGH ARCH BRIDGE

4.1 Outline of seismic retrofitting method

From analytical results, it was recognized that this bridge needs to control the seismic demand since the structural damage by the fault displacement is so large. Then we tried to improve the seismic response using two retrofitting methods, that is, the installation of buckling-restrained brace (BRB) and the modified box and I-section with the increment bending stiffness at the intersections of the arch rib and the stiffened girder. BRBs are used recently as a structural control device in bridge structures. BRBs in this paper were assumed to have a stress-strain property, Young's modulus E=213GPa and E'/60 as shown in Fig.12 and Table 2 shows the cross section area of BRB. BRBs are installed at the locations of bold line in Fig.13 instead of damaged members. In order to increase the bending stiffness about Y-axis rotation, the thickness of web plates for arch ribs and stiffened girder was changed from 1.2 cm to 5.6 cm.

4.2 Distribution of plastic zones of seismic retrofitting model

Fig.14 illustrates the yielded members (red line members) of the seismic retrofitting models with BRBs and incremental stiffness in transverse direction when 3.0 m relative displacement was applied. Though the yielded members of the seismic retrofitting model were able to reduce in comparison with results of the original model, there are some yielded members at the intersections of the arch rib and the stiffened girder, and it is not sufficient for the seismic demand which all members are elastic. It is necessary to propose the more suitable seismic retrofitting method for the fault displacement.

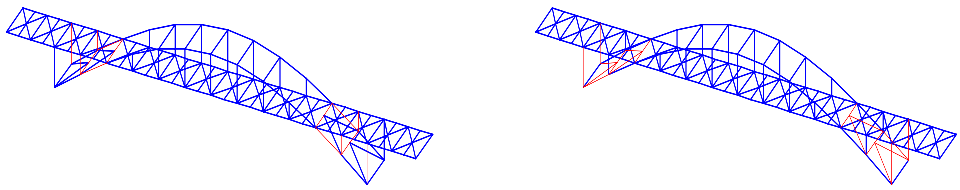

(a) (b)

Figure 14 : Yield members in transverse direction (3m) : (a)BRB model, (b) Incremental stiffness model

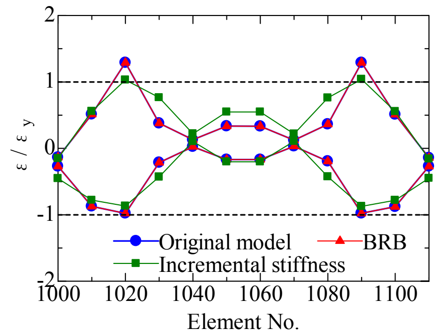

Shrinking direction

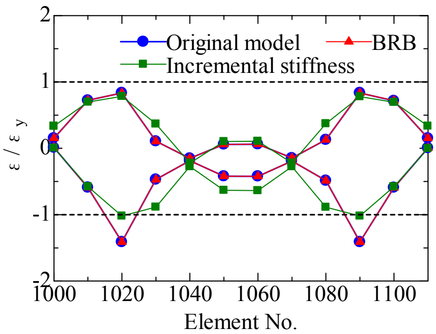

Expanding direction

(a)

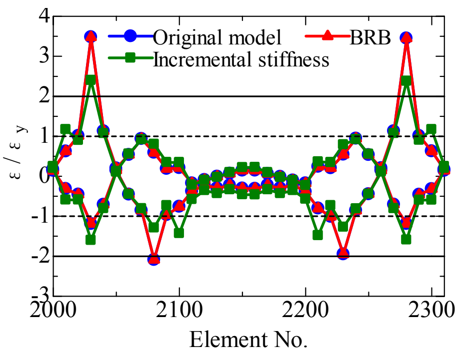

Shrinking direction

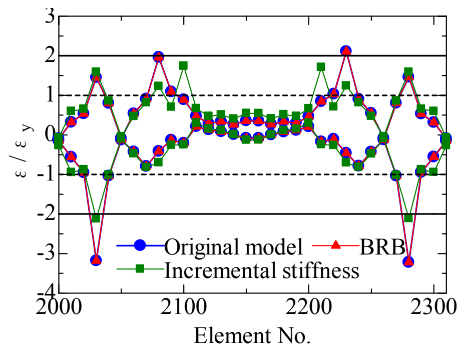

Expanding direction

(b)

Figure 15 : Distributions of maximum and minimum plastic ratios of strain responsein longitudinal direction : (a) Arch rib, (b)Stiffened girder

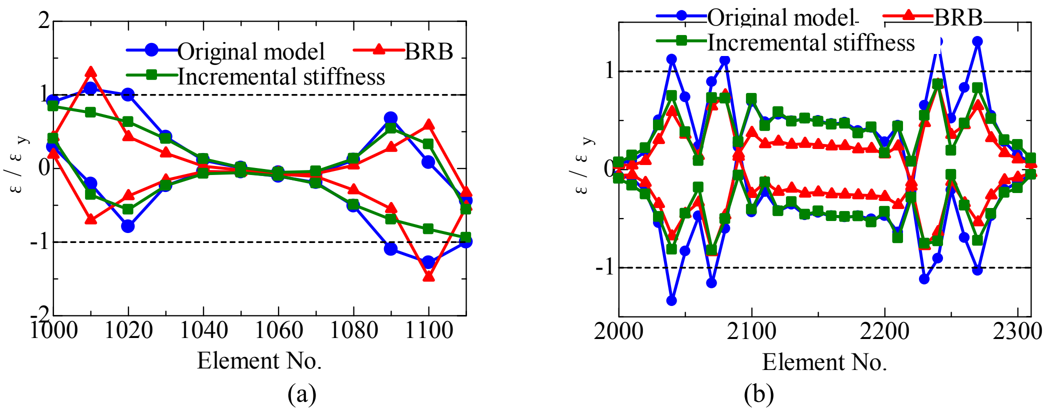

Figure 16 : Distributions of maximum and minimum plastic ratios of strain response in transverse direction

4.3 *Distribution of maximum and minimum plastic ratios of strain*

Fig.15 shows the distribution of the maximum and the minimum plastic ratios of strain response of the arch rib and the stiffened girder in longitudinal direction. From these figures, it can be recognized that the effect of the seismic retrofitting method with the incremental stiffness on the maximum and minimum strain response of the arch ribs in longitudinal direction was large and its value $\varepsilon/\varepsilon_y$ was equal to or less than 1.0. However, the effects of the seismic retrofitting method with BRBs were not able to be seen. This caused by the relatively small ground motion and the dominant seismic behavior of the fault displacement. Fig.16 illustrates the distribution of the maximum and the minimum plastic ratios of strain response of the arch rib and the stiffened girder in transverse directions. It was found that the maximum and the minimum plastic ratios ($\varepsilon/\varepsilon_y$) of strain response of the arch rib and the stiffened girder were not more than 1.0 by the seismic retrofitting method with the incremental stiffness.

5 CONCLUSIONS

Seismic behavior of the half-through steel arch bridge subjected to fault displacement including ground motions in transverse and longitudinal directions were investigated by dynamic response analyses. In dynamic response analyses, the loading conditions were adjusted by controlling two different fault displacement waves at both ends of stiffened girders and at both springings of arch ribs. The seismic behavior of the bridge model subjected to the fault displacement including ground motion was investigated. Finally, in order to control the seismic demand of a half-through steel arch bridge, the seismic retrofitting methods were proposed and we discussed the effect of the proposed methods on the seismic behavior of the bridge model. The conclusions of this study are summarized as the followings.

(1) The effect of the fault displacement wave direction on the damage of the half-through steel arch bridge model is dominant;

(2) The results obtained from dynamic response analyses indicate that the plastic members are clustered near the joints of the arch ribs and stiffened girders. This is caused by the large deformation at this intersection zones;

(3) The effect of the seismic retrofitting method with the incremental stiffness on the maximum and minimum strain response of the arch ribs in longitudinal or transverse directions was large and its value $\varepsilon/\varepsilon_y$ was equal to or less than 1.0;

(4) The effects of the seismic retrofitting method with BRBs on the controlling the seismic demand of the half-through steel arch bridge subjected to fault displacement including ground motions were not able to be seen.

REFERENCES

Japan Society of Civil Engineering. 1999a. The 1999 Ji-Ji Earthquake，Taiwan-Investigation into Damage to Civil Engineering Structure.

Japan Society of Civil Engineering. 1999b. The 1999 Kocaeli Earthquake，Turkey-Investigation into Damage to Civil Engineering Structure.

Japan Road Association. 2002. Specifications for Highway Bridges, Part II Steel Bridge and Part V Seismic Design. (in Japanese)

NIPPON TDAPIII. 2005. Ver2.13 User Manual.

Yamao, T., Takaji T. and Atavit S. 2006. Ultimate strength and behavior of deck-type arch bridges with curved pair ribs, Proc. of Fourth International Conference on New Dimensions in Bridges, Flyovers & Elevated Structures, Fuzhou, China, p.317-324.

Yamao, T., Sho T., Murakami S. and Mazda T. 2007. Seismic behavior and evaluation of seismic performance of half through steel arch bridges subjected to fault displacement, Journal of Seismic Engineering , p.317-324.